Preprint
UCRL-JC-152975

Correlation wave-front sensing algorithms for Shack-Hartmann-based Adaptive Optics using a point source

Lisa A. Poyneer

May 6, 2003

U.S. Department of Energy
Lawrence Livermore National Laboratory

This work was performed under the auspices of the U.S. Department of Energy by the University of California, Lawrence Livermore National Laboratory under contract number W-7405-ENG-48.

Correlation wave-front sensing algorithms for Shack-Hartmann-based Adaptive Optics using a point source

Lisa A. Poyneer
Lawrence Livermore National Lab, Livermore, CA 94550 USA

Abstract

Shack-Hartmann based Adaptive Optics system with a point-source reference normally use a wave-front sensing algorithm that estimates the centroid (center of mass) of the point-source image 'spot' to determine the wave-front slope. The centroiding algorithm suffers for several weaknesses. For a small number of pixels, the algorithm gain is dependent on spot size. The use of many pixels on the detector leads to significant propagation of of read noise. Finally, background light or spot halo aberrations can skew results. In this paper an alternative algorithm that suffers from none of these problems is proposed: correlation of the spot with a ideal reference spot. The correlation method is derived and a theoretical analysis evaluates its performance in comparison with centroiding. Both simulation and data from real AO systems are used to illustrate the results. The correlation algorithm is more robust than centroiding, but requires more computation.

1. Introduction

Shack-Hartmann Adaptive optics (AO) systems use an array of lenslets in the pupil plane to sense the gradient of the wavefront phase across each lenslet area on the pupil. This is done by forming an image of the point source as a 'spot' on the wave-front sensor (WFS) CCD. The spot's shift off null (or off a reference location) determines the average slope of the phase in the lenslet. The location of the spot is normally determined by calculating the centroid (center of mass) of the spot. This method is fast, especially for small numbers of pixels per subaperture spot image, and is in widespread use. It suffers from a number of problems, all of which have been observed anecdotally. In the astronomical AO case, where most systems use 2×2 pixels per subaperture, the gain of the slope estimate changes as the spot size changes. This has been observed in practice[1] and analyzed with an eye towards compensation.[2] When the WFS is not well aligned or is run off-null, this phenomenon can lead to very poor slope estimates.

A second recognized problem with centroiding is that it is susceptible to noise. This is a reason why astronomical AO systems do not normally use 4×4 pixel subapertures. Many systems, such as the laser and vision AO systems which are examined in this paper, use many pixels across each subaperture and could suffer from excessive noise on the slope estimates.

A third downside to centroiding is that is the spots on the WFS camera have any significant aberrations from a diffraction limited spot, the centroid answer will be biased. The most common case of this is background light. This reduces the estimate gain. A less-common problem is when features such as lumps, bulges or secondary spots appear in the WFS CCD. These features will also bias the centroid estimate.

The quality of slope estimates have a significant impact on overall AO performance. Are there better options for slope finding? Work has been done analyzing the problem using estimation theory.[3] Another option is to use a correlation-based method of wavefront sensing, which is discussed in the next section.

2. The correlation technique

The correlation algorithm for wave-front sensing evolved from use in the solar AO community to estimates slopes from images of solar granulation.[4,5] Recent work has expanded this technique to a generalized scene-based wave-front sensing method.[?] This work establish the technique in the case of an arbitrary observed scene, showing that correlation between two subaperture images was the minimum mean-squared-error answer. This correlation can be computed, with negligible loss of estimation performance, by using discrete Fourier transforms. The peak of the correlation function is estimated using parabolic interpolation with three points across the maximum. The performance of this algorithm was be rigorously analyzed, producing theoretical results for the behavior of the algorithm dependent on scene content and illumination type and level. The detailed analysis is summarized here for the special case of applying the scene-based techniques to point sources. In these cases, a reference image of an ideal gaussian spot (or other theoretical profile) is used for the correlation calculation. The main impact of using a fixed, deterministic reference is that the estimate variance is drastically reduced from the case where a new, noisy reference is used at each time step.

This technique, called correlation for simplicity in the point-source case, is fundamentally different than centroiding. The center of mass is calculated by weighting the pixels relative to their distance from the center. In the general case the pixels furthest from the center have the least signal, but they have the highest weighting. This makes centroiding susceptible to both noise and spot abnormalities, as will be shown below. Correlation compares the spot image to a reference spot. The values used for the estimate are around the location of best fit, where the portions of the spot with the most signal are weighted highest. This causes the correlation algorithm to be much less sensitive to noise, as will be derived below. It also makes it insensitive to background light and most spot abnormalities. This fundamental difference in the two WFS algorithms is illustrated in Fig. **??**. (It is worth noting that the methods are incompatible - centroiding can not be implemented as a correlation with an image.) The next sections give a thorough theoretical analysis of the centroiding and correlation algorithms.

3. Statistical analysis of centroiding techniques

A centroiding algorithm is defined for this paper as an algorithm that calculates the center of mass (the centroid) of the spot seen in a subaperture to estimate the shift off-null. To analyze the performance of centroiding methods, we use the following model. The analysis will be done for the x-shift only; the y-shift case involves simply a flipping of indices.

The subaperture image $s[i,j]$ on the CCD is $N \times N$ pixels across, where N is generally an even number. At its most basic, the centroider scales and adds all the pixels on the right hand side (positive direction), subtracts off a similar weighting for the left hand side, and divides by the sum of all the pixels. In this case, where r is the sum of the right side, l for the left and t the sum of all

the pixels, the centroid estimate is

$$\hat{x} = \frac{r - l}{t}. \tag{1}$$

Because $\hat{x}$ is a quotient, if we do not have full knowledge of the probability distributions of r, l and t we cannot obtain the statistics of $\hat{x}$. However, linearizing the equation allows evaluation of the mean and variance of $\hat{x}$ with knowledge of only the means and variances of r, l and t. This approximation is a minor one and Monte Carlo simulations show close accord between this approximation and the true statistical results. With use of partial derivatives, the expression for $\hat{x}$ is

$$\hat{x} = \frac{r}{m_r} - \frac{l}{m_l} - \frac{t(m_r - m_l)}{m_t^2} + \frac{m_r - m_l}{m_t}, \tag{2}$$

where the m terms are the means of the random variables. The expectation of the estimate is

$$\mathrm{E}[\hat{x}] = \frac{m_r - m_l}{m_t} \tag{3}$$

Evaluating the variance of this expression produces

$$\mathrm{Var}(\hat{x}) = \frac{\sigma_r^2 + 2m_r^2 + \sigma_l^2 + 2m_l^2 - 4m_r m_l}{m_t^2} + \frac{\sigma_t^2 (m_r - m_l)^2}{m_t^4} + \frac{2(m_r - m_l)}{m_t^3}(\mathrm{E}[lt] - \mathrm{E}[rt]) \tag{4}$$

Now the random variables r, l and t must be defined. Where $s[i, j]$ is the random vector of the subaperture image, the basic centroiding algorithm produces terms that are expressed as

$$r = \sum_{i=N/2}^{N-1} \sum_{j=0}^{N-1} (i - N/2 + 1/2) s[i, j], \tag{5}$$

$$l = \sum_{i=0}^{N/2-1} \sum_{j=0}^{N-1} (-i + N/2 - 1/2) s[i, j], \tag{6}$$

and

$$t = \sum_{i=0}^{N-1} \sum_{j=0}^{N-1} s[i, j]. \tag{7}$$

Now a statistical model of the received image must be defined. For this model, each pixel is assumed to have a poisson-distributed count of photo electrons with parameter $\lambda[i, j]$. This parameter vector describes the profile of the spot, for example how wide it is and any aberrations away from being radially symmetric. To this profile is added white read noise of a gaussian distribution with zero mean and variance σ_n^2. In this case the means and variances of r, l, t are (recognizing that $\sum_{i=N/2}^{N-1} (i - N/2 + 1/2)^2 = N^2(N^2 - 1)/24$)

$$m_r = \sum_{i=N/2}^{N-1} \sum_{j=0}^{N-1} (i - N/2 + 1/2) \lambda[i, j], \tag{8}$$

$$\sigma_r^2 = \sum_{i=N/2}^{N-1} \sum_{j=0}^{N-1} (i - N/2 + 1/2)^2 \lambda[i,j] + \frac{N^2(N^2-1)}{24}\sigma_n^2, \tag{9}$$

$$m_l = \sum_{i=0}^{N/2-1} \sum_{j=0}^{N-1} (i - N/2 + 1/2)\lambda[i,j], \tag{10}$$

$$\sigma_l^2 = \sum_{i=0}^{N/2-1} \sum_{j=0}^{N-1} (-i + N/2 - 1/2)^2 \lambda[i,j] + \frac{N^2(N^2-1)}{24}\sigma_n^2, \tag{11}$$

$$m_t = \sum_{i=0}^{N-1} \sum_{j=0}^{N-1} f\lambda[i,j], \tag{12}$$

$$\sigma_t^2 = \sum_{i=0}^{N-1} \sum_{j=0}^{N-1} \lambda[i,j] + N^2\sigma_n^2 \tag{13}$$

The estimate variance is the sum of two separate terms: the base level due to photon noise, and the term due to read-noise only. First we will examine the term due only to photon noise. For the zero-shift case when $m_r = m_l$, this drastically simplifies to:

$$\mathrm{Var}(\hat{x})_p = \frac{\sigma_r^2 + \sigma_l^2}{m_t^2}. \tag{14}$$

If we change the total number of photons received in a uniform multiplicative manner by a constant f, both the mean and variance will also change by the factor f. This produces a new equation

$$\mathrm{Var}(\hat{x})_p = \frac{\sigma_r^2 + \sigma_l^2}{f m_t^2}. \tag{15}$$

which is an inverse-power relationship. Normalizing m_t such that f is the total number of photo-electrons received, the signal-to-noise-ratio (SNR) is simply $\sqrt{f}$. Now the standard deviation of the estimate (and of its error) is inversely proportional to the SNR:

$$\mathrm{StDev}(\hat{x})_p = \frac{\left(\sigma_r^2 + \sigma_l^2\right)^{1/2}}{m_t\sqrt{f}}. \tag{16}$$

This result agrees with prior derivations for centroid algorithms. The actual performance depends on the spot profile (or shape) as determined by $\lambda[i,j]$. For a given profile, as the amount of light changes, the estimate variance follows in a regular manner.

The second part of the estimate variance is the part due to read noise. Using the result from above, the general formula is now:

$$\mathrm{Var}(\hat{x}) = \mathrm{Var}(\hat{x})_p + \sigma_n^2 \left(\frac{2N \sum_{i=N/2}^{N-1} (i - N/2 + 1/2)^2}{m_t^2} + \frac{N^2(m_r - m_l)^2}{m_t^4} \right) \tag{17}$$

The best-case response to read noise occurs when the spot is is driven to null in closed loop and $m_r - m_l = 0$. The equation then simplifies to a function of N,

$$\mathrm{Var}(\hat{x}) = \mathrm{Var}(\hat{x})_p + \sigma_n^2 \left(\frac{N^2(N^2-1)}{12 m_t^2} \right). \tag{18}$$

This formula clearly shows the deleterious effects of having more pixels on the centroiding algorithm. For an $N \times N$ subaperture image, the estimate variance goes as N^4, or the square of the total number of pixels on the detector. Table 1 shows the multipliers for various size subapertures.

N(pixels)	Noise Multiplier
2	$1/m_t^2$
4	$20/m_t^2$
6	$105/m_t^2$
8	$336/m_t^2$
10	$825/m_t^2$
12	$1716/m_t^2$
14	$3185/m_t^2$
16	$5440/m_t^2$

Table 1. Noise multipliers for centroiding, for varying number of pixels N.

The second down-side to using a centroid algorithm comes from its response to background light. Even small amounts of background light can have significant effects of the estimate of the centroid location. If a source of background light that has uniform expected value b at each pixel is present, the resulting estimate expectation is now

$$\mathrm{E}[\hat{x}] = \frac{m_r - m_l}{m_t + N^2 b}. \tag{19}$$

This is independent of the variance of the background source. The background lowers the gain of the wavefront sensor algorithm. The gain (which is 1 if there is no background b) is

$$\mathrm{gain} = \frac{m_t}{m_t + N^2 b}. \tag{20}$$

This means that the gain of the centroid algorithm drops to 50% if there is a uniform background level of m_t/N^2 per pixel. The more pixels there are, the more sensitive the centroiding algorithm is to background.

Background also has an effect on the variance of the estimate and its read noise multiplier. Having an excess background of level b modifies both $\mathrm{Var}(\hat{x})_p$ and the noise multiplier by a factor of $[m_t/(m_t + N^2 b)]^2$. So the addition of background to a subaperture will reduce both the estimate gain and the variance. Similarly, removing a background will increase both the estimate gain and the variance. So background subtraction with centroiding will increase the overall estimate variance. This is a zero-sum situation - leaving in the background reduces the noise propagation, but it reduces the estimate gain by the same factor.

4. Statistical analysis of correlation techniques

The performance of the correlation algorithm can also be analyzed. Again, the signal $s[i,j]$ is the subaperture image being analyzed. The correlation technique uses a fixed, deterministic reference $r[i,j]$, which is typically a gaussian spot profile. Using our preferred method of interpolation, with a single slice through the correlation peak, the expectation of the estimate is

$$\mathrm{E}[\hat{x}] = \frac{0.5(m_1 - m_{-1})}{m_1 + m_{-1} - 2m_0}. \tag{21}$$

The variance of the estimate is, in the most general case,

$$\begin{aligned} \mathrm{Var}(\hat{x}) \quad = \quad & [\sigma_{-1}^2(m_1 - m_0)^2 + \sigma_0^2(m_{-1} - m_1)^2 + \sigma_1^2(m_0 - m_{-1})^2 \\ & +2(m_1 - m_0)(m_{-1} - m_1)\sigma_{-1,0}^2 + 2(m_1 - m_0)(m_0 - m_{-1})\sigma_{-1,1}^2 \\ & +2(m_{-1} - m_1)(m_0 - m_{-1})\sigma_{0,1}^2][m_{-1} + m_1 - 2m_0]^{-4}. \end{aligned} \tag{22}$$

In the zero-shift case, assuming a symmetric reference, this reduces to a more simple expression

$$\mathrm{Var}(\hat{x}) = \frac{\sigma_1^2 - \sigma_{-1,1}^2}{8(m_0 - m_1)^2} \tag{23}$$

The terms in the above equations $(m_k, \sigma_k^2, \sigma_{k,l}^2)$ are the means, variances and covariances of the cross-correlation. Written out in terms of the reference image $r[i,j]$ and the subaperture pixel means and variances $m_s[i,j]$ and $\sigma_s^2[i,j]$, they are:

$$m_k = \sum_{i=0}^{N-1}\sum_{j=0}^{N-1} r[i-k,j]m_s[i,j], \tag{24}$$

$$\sigma_k^2 = \sum_{i=0}^{N-1}\sum_{j=0}^{N-1} r^2[i-k,j]\sigma_s^2[i,j], \tag{25}$$

and

$$\sigma_{k,l}^2 = \sum_{i=0}^{N-1}\sum_{j=0}^{N-1} r[i-k,j]r[i-l,j]\sigma_s^2[i,j], \tag{26}$$

where for simplification of notation the reference signal is assumed to be periodic with period N.

These equations can be interpreted in a similar manner to those for the centroiding case. The same model as above will be used, with each pixel being the sum of independent poisson-distributed counts from the point-source and zero-mean white gaussian noise of variance σ_n^2 (i.e. $m_s[i,j] = \lambda[i,j], \sigma_k^2[i,j] = \lambda[i,j] + \sigma_n^2$). The estimate variance is now the sum of two independent terms. Assuming again the photoelectron scaling factor f, the estimate variance due to photon noise becomes, in the zero-shift case,

$$\mathrm{Var}(\hat{x})_p = \frac{\sigma_1^2 - \sigma_{-1,1}^2}{8f(m_0 - m_1)^2}. \tag{27}$$

This is, like the centroider, an inverse relationship between the standard deviation of the estimate and the SNR ($\sqrt{f}$)

$$\mathrm{StDev}(\hat{x})_p = \frac{(\sigma_1^2 - \sigma_{-1,1}^2)^{1/2}}{\sqrt{f}\sqrt{8}(m_0 - m_1)}. \tag{28}$$

This inverse relationship also holds for the general case, though we will not give the long expression. In practice the coefficients to the SNR law for estimate standard deviation are quite close for the correlation and centroider methods.

As for the portion of the variance due to the read noise, it also has a long expression in the general case. In the zero-shift case it is simpler:

$$\mathrm{Var}(\hat{x})_r = \sigma_n^2 \frac{\sum_{i=0}^{N-1}\sum_{j=0}^{N-1} r[i-1,j](r[i-1,j] - r[i+1,j])}{8(m_0 - m_1)^2}. \tag{29}$$

For the centroider, the noise multiplier depends only on the number of pixels N and the mean number of photons received m_t. For the correlation algorithm the noise multiplier depends on both the structure of the subaperture image received $(m_0 - m_1)$ and on the reference used. There is no direct dependence on the number of pixels. In practice, the noise multiplier for the correlation algorithm can be orders of magnitude less than the centroider. The noise multiplier is also related to the inverse-square of the total amount of light received, as the centroider is. In this case, by including the factor f from above to control the total amount of light received, the noise multiplier is proportional to $1/f^2$. So both noise multipliers follow a sensible SNR relation - the more signal present, the less the noise gets through to the estimate.

As for the effect of background, adding a mean background level b to each pixel has no effect on the expected value of the estimate. All the b terms in Eqn. 21 cancel out, leaving the estimate independent of background level. If the background is a constant factor added in (or taken away), the estimate variance is also independent of the amount b. This is because b appears only in m_k terms, all of which come in matched difference pairs in the relevant equations, leading to cancellation of all b terms. Therefore the background level (if constant) is irrelevant to correlation performance.

5. Performance comparison: astronomical AO system

Most astronomical AO systems operate with quadcell detectors. Exceptions include the Lick AO system, which can operate in 4×4 mode, and the PALAO system before its very recent upgrade. In some cases the system may be limited by CCD quality in terms of read noise and data rate. The quadcell algorithm does not suffer from read-noise blowup like larger centroiders. However, it does suffer from lost light. In particular, as the spot size on the detector increases, light is lost off the edges of the center pixels. This phenomenon manifests itself as a reduced centroid estimate gain. This problem is particularly bad when the WFS is run off-null.

This gain problem could be fixed by going to 4×4 pixels. Centroiding on more pixels greatly reduces this variable gain problem as spot size changes. However, the estimate variance will increase due to the extra pixels. The correlation algorithm provides the benefits of both methods. It has a very stable gain as spot size changes, but it much less sensitive to read noise than the centroider.

Below we present analytic and simulation results for this specific test case. We first discuss the exact algorithms used, then compare algorithm performance for a variety of conditions. For

x	y	y	x
y	z	z	y
y	z	z	y
x	y	y	x

Fig. 1. The fixed reference 'spot' used for correlation in the 4×4 case. It can be parameterized by a single number $k = (z - y)/(y - x)$, which governs the width of the spot. The bigger k is, the narrower the spot.

our spots we chose an underlying gaussian profile, which was shifted by given amounts, sampled at high resolution and binned down to generate the simulated CCD images.

For this comparison, we used a WFS that had 4×4 pixels for each subaperture. The center 2×2 pixels were used for the classic quadcell algorithm. All 16 were used for a centroider and for the correlation algorithm. The correlation method used a fixed reference. This symmetric reference in illustrated in Fig. 1. In this small case, the circular spot reference can be parameterized by a single number. This constant k is simply the ratio of the slopes: $k = (z - y)/(y - x)$. Performance does vary with k, but there is a large operating range for k that gives satisfactory results.

The first behavior studied was the response to changing spot size for non-zero shifts. A plot between algorithm gain for the slope estimate and the spot size is shown in Fig. 2. When the spot's width is effectively smaller than a pixel, the WFS configuration is non-linear. No algorithm will accurately locate a spot that is smaller than a pixel when it is shifted off null. In the well-sampled range, the quadcell gain dropped off significantly as spot size increased. In the range of spot FWHM from just over 1.0 pixels to 2.0 pixels, where the correlation algorithm and the centroider have smooth response, the quadcell gain drops by a factor of 3. Using 4×4 pixels makes the response much smoother.

The second important behavior is response to read noise. As derived above, the noise mulitplier in the zero-shift case for the quadcell case was $1/m_t^2$, whereas the noise multiplier for the 4×4 centroider was $20/m_t^2$. Both are independent of the actual spot size. The noise multiplier for the correlation algorithm depends on both the type of reference (controlled by the factor k) and the actual spot profile. Where C_1 and C_2 are two numbers dependent on the image profile, the noise multiplier is a function of k:

$$\text{noise mult.} = \frac{0.5(1 + k^2)}{(C_1 + C_2 k)^2}. \tag{30}$$

For a wide range of spot sizes in this case, $C_2 \gg C_1$ holds. This produces a relatively constant noise multiplier for $k > 3$ that is asymptotically approaching $0.5(C_2)^{-2}$. As the spot size on the detector increases, the noise multiplier increases as well (for a constant total number of photoelectrons received.) The noise multipliers for all three algorithms at varying spot size are presented in Table 2 . In this case, the noise multiplier for correlation is only 2 to 3 times that of the quadcell. The centroider is 10 to 25 times bigger, depending on the spot size. These result are confirmed by simulation. Fig. 3 shows Monte Carlo simulation results for a specific test case: 1.25 pixel FHWM

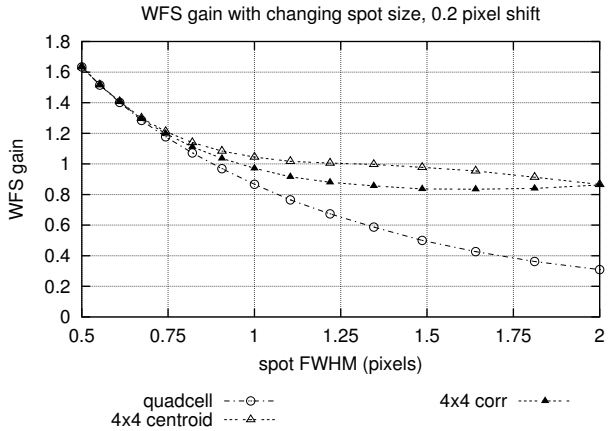

Fig. 2. Changing spot size adversely effects the gain of the quadcell algorithm. This is due to light lost off the edges of the pixel and the spot size grows. Both the 4×4 centroider and the correlation algorithms have close to constant gain once the spot is adequately sampled, though the centroider starts to lose accuracy as the spot size becomes quite large.

spot of 200 counts with a 0.2 pixel shift in the x-direction. The standard deviation of the shift estimate was determined, and it was normalized by the gain of the estimate, because the three methods all had different gains. With this normalization, the correlation method has a very similar response to read noise as the quadcell, despite having 4 times as many pixels. The 4×4 centroider performance degrades at a much faster rate. This test case has shown the following: shift estimate gains are more closely constant with changing spot size when 4×4 pixel subapertures are used. However, the read noise propagates through the centroider algorithm at a much higher rate than the other methods. The correlation method has relatively constant gain on the estimate, while having response to read noise comparable to that of the quad cell.

In a very well-aligned system operating on-null, the variable gains of the quadcell would not be a serious problem. However, if the spots cannot be reliably driven to null and a larger detector is available, using the correlation algorithm with 4×4 pixel subapertures is a very good solution.

spot FWHM (pixels)	Quadcell	Noise Mult. Centroider	$\times 10^{-5}$ Correlation
0.5	2.50	50.0	5.05
0.75	2.52	50.0	5.10
1.0	2.70	50.0	5.63
1.25	3.19	50.0	7.26
1.5	4.07	50.0	10.6
1.75	5.33	50.0	16.5

Table 2. Noise multipliers for the three algorithms. For each case the total number of photoelectrons received on the entire 4×4 pixel detector is set to 200. The quadcell noise multiplier increases because less light is received in the center pixels as spot size increases. The correlation noise multiplier is calculated for $k = 10$.

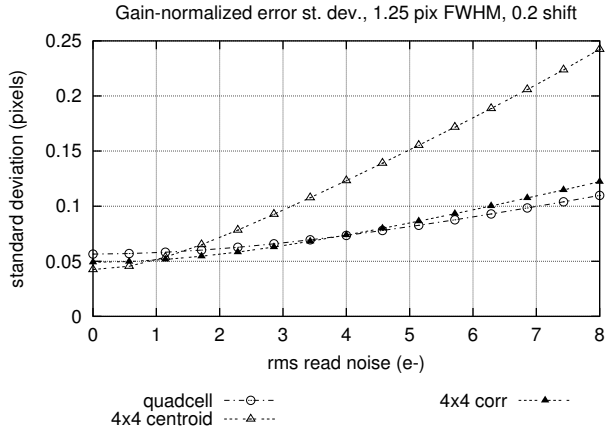

Fig. 3. Estimate standard deviation versus read noise. The standard deviation of is normalized to the estimate gain. The 4×4 centroider has significantly high noise propagation.

6. Performance comparison: Vision AO

Many AO systems, particularly those for vision-related applications, use subapertures with large numbers of pixels. For our test case we chose the UC Davis/LLNL vision system. It has spots with a FWHM of approximately 3.1 pixels spaced every 12.7 pixels apart on the WFS camera. Typical background levels are 19-20 counts per pixel. Our data sets had 1300-1500 counts from the point source per subaperture. Based on this information, some general predictions can be made. The correlation reference was chosen to be a gaussian spot with 3.0 pixel FWHM. Based on theory for the zero-shift case, the behavior of the estimate variance was determined. The results are given in Table 3. These numbers show that if the only noise source were photons, the centroiding method would have lower rms error than the correlator. The background-subtracted centroider is 23.8 times more sensitive.

We obtained a set of 50 exposures with no aberration in the system, and another set of 50 with a .25 diopter aberration. We took two approaches with the data. The first was to predict how performance would vary due to background levels, in particular the estimate gain and noise multipliers.

Based on the background and signal counts, we can predict the difference in estimate gains between basic centroiding and use of background subtraction. From the .25 diopter data we determined that $m_t = 1322.$ and $b = 19.3$. Using Eqn. 20, this means the slope estimate with basic centroiding would be only 32.2% of the estimate obtained when the background is subtracted out first. Then the actual gains of the algorithms were determined by taking the mean slope estimate for each subaperture, reconstructing the phase and determining the rms of the focus. Doing so reveal that the basic centroider has a gain of 34.9%. This test was repeated for the reference (no aberration) set. Electron count calculations led to a prediction of a gain of 35.1%. Because the spots are not spaced a whole number of pixels apart, the parsing of the CCD pixels introduces a focus term. The rms value of this reconstructed focus produced a gain of 33.2%. These data analyses agree with our theoretical predictions as to the effect of background on slope estimate gain.

The second behavior that we analyzed was the standard deviation of the estimates for the three different algorithms. This was done by analyzing each subaperture through time. The average results (across all subapertures) for the standard deviation of the x- and y-estimates are shown in Table 4. These results show several phenomena. The basic centroider, which is known to have a significantly lower gain, also has a very low standard deviation of around 4 thousandths of a pixel.

Method	StDev$(\hat{x})_p$ pixels 10^{-3}	Noise Mult. 10^{-5}
Centroider	11.9	10.3
Cent. Back Sub	37.4	102.
Correlation	45.2	4.28

Table 3. Predicted error variance components for the three algorithms, based on a model of Davis Vision AO system WFS.

St. Dev	**No Aberration**		
10^{-3} pixels	Centroid	Cent Back Sub	Correlation
x-slope	3.77	10.8	5.45
y-slope	4.13	11.9	6.57
gain norm.			
x-slope	16.4	15.4	5.45
y-slope	18.0	16.9	6.57
St. Dev	**.25 Diopter**		
10^{-3} pixels	Centroid	Cent Back Sub	Correlation
x-slope	3.70	12.1	5.90
y-slope	3.90	12.5	6.20
gain norm.			
x-slope	14.7	16.4	5.90
y-slope	15.5	17.0	6.20

Table 4. Average subaperture estimate standard deviation, no aberration case. Using gain estimates, the standard deviations are normalized so all methods have equivalent gains.

It is inaccurate, but very consistently so. The centroider with background subtraction should differ by the pre-determined factor (calculated above) based on counts. For the no aberration case this factor was predicted to be 35.1%. The slope estimate standard deviation has a difference of 34.7% for x-slopes and 34.9% for y-slopes. For the .25 diopter case, the prediction was 32.2%. For x-slopes the standard deviation had a difference of 30.6%; for y-slopes it was 31.2%.

The centroider algorithm (either flavor) has 16 thousandths of a pixel rms error when gain-normalized to the correlation result. The correlator has only 6 thousands of a pixel rms error. The correlator has, for these data sets, 2.7 times less rms error on the estimate than the centroiding methods. This significant difference indicates that the SNR of these data sets is quite low, most likely due to excessive noise on the WFS camera. In a high SNR situation, the performance of both methods should be much more similar.

7. Performance comparison: AO control of a laser

The Solid state heat capacity laser (SSHCL) AO system does intracavity correction of a high-power unstable resonator laser. The AO system has some unique features that have posed problems for wave-front sensing. A very noticeable effect is that the spots on the WFS CCD frequently have significant shape deformations (or even splitting). For our tests we analyzed the WFS camera data using 12×12 pixel subapertures.

Based on analysis of the WFS data, a model was developed for-well behaved spots. The spots have an underlying gaussian profile (as determined by fitting) of approximately 2.5 pixels FWHM. A typical image will have 8 counts of background per pixel and 1000 counts in the spot itself. A reference spot of 2.0 pixels FWHM had the best performance for the correlation method. Just as with the Vision AO system, theoretical predictions of the estimate quality are possible given this model. For the zero-shift case, the estimate variance properties of the three algorithms are given in Table 5. Again, the estimate standard deviation for the gain-adjusted centroider and the correlator are reasonably close. The noise multipliers are drastically different. The basic centroider has a noise mulitplier 12.7 times greater than the correlator. The background-subtracted centroider has a multiplier 58.7 times greater than the correlator.

Just as with the Vision AO system, background light is a significant problem. This makes the centroider inaccurate for even well-formed spots. Using the formula dervied above (Eqn. 20), the gain loss due to background can be explicitly computed. Given the range of m_t (total counts in the spot) for the exposures, this results in a gain of 35% - 55% of normal. This result was confirmed by actually computing the slopes for a series of spots with both methods and comparing them.

The more challenging problem is that many spots are not well-formed at all. WFS images show that spots can have significant secondary lumps which are frequently nearly 50% of the peak intensity of the central core. These lumps throw off the centroider, and drastic thresholding is required to remove them and obtain accurate slope estimates. This thresholding involves finding the maximum pixel value in the subaperture and setting a threshold to a specified percentage of that level. All pixels below that threshold are set to zero. All pixels above the threshold are kept, with the threshold value subtracted off to remove background effects. (Thresholding is discussed further in the following section.) Shown in Fig. 4 is a poor-quality spot that is analyzed with increasing thresholds. All pixels below a specific percentage of the peak value for that subaperture are zeroed

Method	$\mathrm{StDev}(\hat{x})_p$ pixels 10^{-3}	Noise Mult. 10^{-5}
Centroider	16.2	37.1
Cent. Back Sub	34.8	172.
Correlation	42.5	2.93

Table 5. Model for algorithm performance for HLSTF scenario. Based on typical spot size and photon and background levels. If there is no read noise, the centroider performance better than the correlation algorithm. Its read noise multiplier is 58.7 times greater, however.

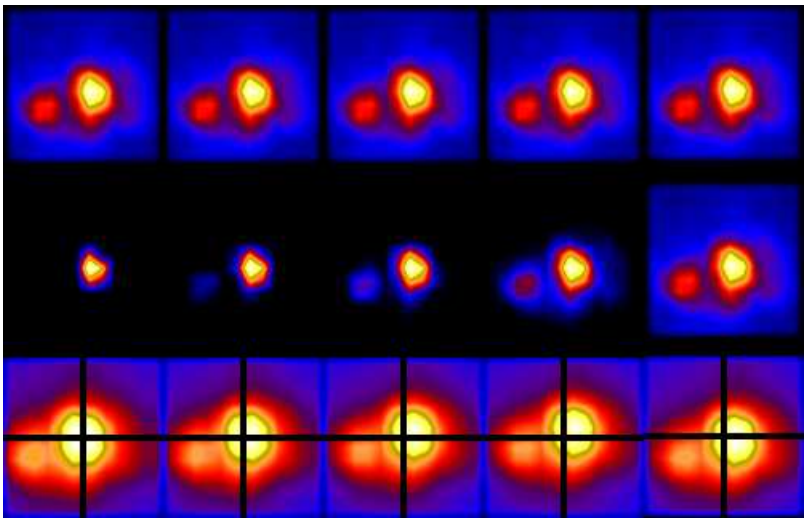

Fig. 4. A single frame of the subaperture data, at different levels of thresholding. From left to right, all data below 50%, 40%, 30%, 20% and 10% of the maximum pixel value were ignored. This masking is shown in the second row. In the bottom row is the center of mass of the spot as obtained with the centroiding algorithm. Both the background and the halo structure have significant impact on the shift estimate, as shown by the cross-hairs.

out. As shown, it takes a drastic level of thresholding to remove secondary lumps that prevent the centroider from finding the center of the spot core.

The correlation algorithm easily surmounts both these obstacles. The algorithm is insensitive to uniform background level. Secondly, using a fixed spot reference (one that is a guassian) actually works very well in matching the central core location of the spot. Secondary lumps are in essence ignored and the best match to the central peak is found. Illustrated in Fig. 5 is the same spot at 6 consecutive shots in open loop. The shape of the spot changes dramatically from shot to shot. Shown in the bottom frames are the center as determined by the correlation algorithm with a gaussian spot as a fixed reference. This method is very good at correctly finding the center of the main core, regardless of aberrations in the halo. Assuming that this center of the core is what we want to locate, the correlation algorithm does a much better job at finding it than the centroiders. Furthermore, analysis indicates that the correlation algorithm will have much better response to noise.

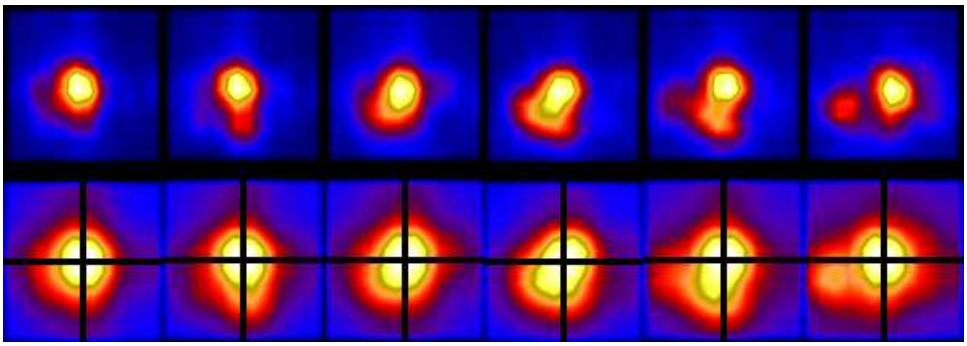

Fig. 5. The same subaperture followed through six laser shots in open loop. On top is the 12×12 pixel spot data, upsampled with linear interpolation for clarity. On the bottom is the spot, sub-pixel shifted to the slope estimate obtained by the correlation method. The cross-hairs clearly is at the center of the spot core for all cases.

8. Conclusions

So... why would you want to use correlation?

- Insensitive to the presence of background.
- Lower read noise propagation (good for noisy detectors).
- Relatively uniform gain with changing spot size (versus quadcell case).
- Robust to aberrations in the spot halo that throw off centroiders.

Why would you not want to?

- It takes longer! Centroiding and variants (thresholding, etc.) are fundamentally $O(N^2)$ algorithms. Correlation, on non-powers-of-2, is $O(N^3)$. If the shift size is constrained, there are work-arounds that are $O(N^2)$ with a large constant in front. Also faster for powers-of-two sizes with FFT.
- AO system is not read-noise limited. Centroiding and correlation have similar performance in the absence of significant read noise. If the error budget can be met with a centroider, why do more computation?

Acknowledgements

Questions?? Contact me at poyneer1@llnl.gov. This paper has not yet been approved for unlimited release outside of LLNL, so take care if you distribute it.

References

1. I. de Pater, S. G. Gibbard, B. A. Macintosh, H. G. Roe, D. T. Gavel, and C. E. Max, "Keck adaptive optics images of Uranus and its rings," Icarus **160**, 359–374 (2002)

2. J.-P. Veran and G. Herriot, "Centroid gain compensation in Shack-Hartmann adaptive optics systems with natural or laser guide star," J. Opt. Soc. Am. A **17**, 1430–1439 (2000)

3. M.A. van Dam and R.G. Lane, "Wave-front slope estimation," J. Opt. Soc. Am. A **17**, 1319–1324 (2000)

4. T.R. Rimmele, "Solar adaptive optics," in *Adaptive Optical Systems Technology,* P.L. Wizinowich; Ed., Proc. SPIE **4007**, 218–231 (2000)

5. T.R. Rimmelle, O. von der Luehe, P.H. Wiborg, A.L. Widener, R.B. Dunn and G. Spence, "Solar feature correlation tracker," in *Active and adaptive optical systems,* M.A. Ealey; Ed., Proc. SPIE **1542**, 186–193 (1991)

6. L.A. Poyneer, R. Sawvel and C. Thompson, "Scene-based wave-front sensing: analysis, simluation and experiment," submitted to Applied Optics, 2003.